ACS Biomaterials SCIENCE & ENGINEERING

pubs.acs.org/journal/abseba

Article

Fabrication of a Perfusable 3D In Vitro Artery-Mimicking Multichannel System for Artery Disease Models

Minkyung Cho and Je-Kyun Park*

Cite This: *ACS Biomater. Sci. Eng.* 2020, 6, 5326−5336

Read Online

ACCESS | Metrics & More | Article Recommendations | Supporting Information

ABSTRACT: Fabrication of a 3D in vitro model that mimics the artery takes an important role in understanding pathological cell behaviors and mechanisms of vascular diseases by proposing an advanced model that can recapitulate a native vessel condition in a controlled manner. Because a model geometry and the structure of cells are significant for the recapitulation of the hemodynamics of arterial and cell functions, it is necessary to mimic geometries and to induce the proper morphology and orientation of the cells when fabricating a model. In this study, smooth muscle cells (SMCs) and endothelial cells (ECs), which were the main elements in the arterial wall, were cocultured in a multichannel device connected with polydimethylsiloxane (PDMS) fluidic chamber modules to parallelly fabricate a pefusable 3D in vitro human artery-mimicking multichannel system. In the coculture model, a circular PDMS channel with a wrinkled-surface guided directionality and contractile morphology to SMCs, and media perfusion induced directionality to a confluent EC layer as in vivo. Protein markers of cells and synthesized extracellular matrices were demonstrated. Because multichannels were connected to a microfluidic module in a device, it was possible to easily control the microenvironmental conditions and to fabricate coculture models in parallel with a single flow system. Coculture models that can be tuned in designs such as diameter, wall shear stress, and geometry of artery disease were constructed by 3D-printed molds to recapitulate various cellular microenvironments and to model vessels effectively. Finally, the effect of wall shear stress on cells was compared using a device with four different degrees of stenosis channels and investigated in parallel.

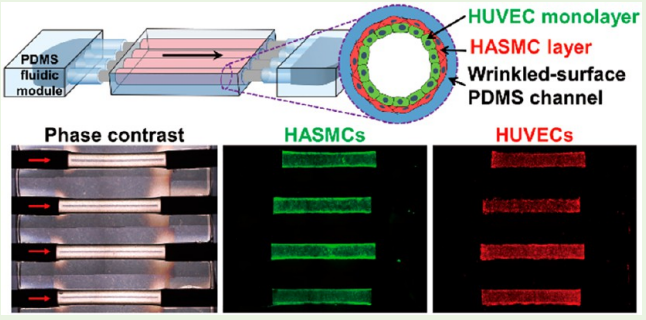

KEYWORDS: *3D in vitro coculture model, 3D-printed mold, endothelial cells, microfluidic module, smooth muscle cells, wrinkled structure*

1. INTRODUCTION

Atherosclerosis is a narrowing of the blood vessel due to the formation of an atheroma on the arterial wall, resulting in various fatal diseases such as myocardial infarction and stroke.[1−6] Therefore, it is important to simulate and study vascular diseases by fabricating an in vitro model that mimics the artery to understand diseases.[7,8] An in vitro artery model recapitulating native vessel geometries as similar as possible can provide clinically relevant physiological conditions that are favorable for analyzing phenomena using this model.[9] Microfluidics is an emerging tool to fabricate an in vitro vessel model[10,11] because it simplifies the mimicking of in vivo characteristics through the capability of 3D cell culture and microenvironmental condition control.[12] Rectangular channel models that are easy to manufacture have been used to date.[13] In recent years, however, studies have been conducted to recapitulate physiological conditions such as fluid flow similar to the native vessel by applying a circular channel geometry similar to in vivo.[9,13−17] Because the structure and orientation of cells are important factors in their function,[18,19] it is necessary to induce proper morphology and orientation of the cells to have functionality when generating an in vitro model.[20] Smooth muscle cells (SMCs), which represent a spindlelike contractile phenotype, are mostly aligned helically or circumferentially in tunica media of the native artery to provide mechanical strength for the role of vasoconstriction and vasodilation.[20−22] In the case of endothelial cells (ECs), they exist as a confluent monolayer in tunica intima, act as a barrier, and are aligned in the direction of blood flow.[20,21,23]

In previous studies that mimicked arteries in vitro, the artery models produced were mostly free-standing models or channel device models with stacked cell layers. Because free-standing models were mainly intended for vascular graft, scaffolds such as hydrogels,[24−26] electrospun membranes,[27−29] and polymers (polypropylene,[7] polydimethylsiloxane (PDMS),[30] polyester,[31] and polyethylene−polycaprolactone (PEG−PCL)[32]) were used, or cell sheets[33,34] were harvested after a long time and

Received: May 19, 2020
Accepted: August 14, 2020
Published: August 14, 2020

https://dx.doi.org/10.1021/acsbiomaterials.0c00748
ACS Biomater. Sci. Eng. 2020, 6, 5326−5336

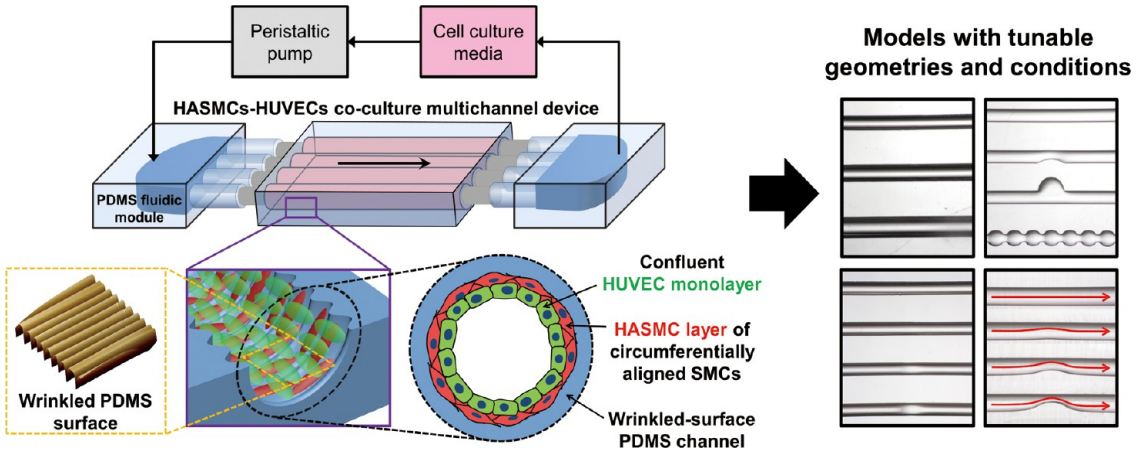

Figure 1. Scheme of a perfusable 3D in vitro artery-mimicking multichannel system. The circumferentially aligned HASMC layer and a confluent HUVEC monolayer were cocultured in wrinkled-surface circular PDMS channels to fabricate models with versatile geometries and conditions.

rolled to produce the model. These methods required that the cell culture took a long time, included an artificial scaffold, or failed to meet cellular orientation. On the other hand, channel device models with cells inside were usually produced for in vitro assay purposes such as thrombosis study, but so far there were only a few cocultured models and there has been no interfacing between a microfluidic module and multichannels.[8,9,11,16,35−37] There was also a channel model that had wrinkles on the surface of the channel to give cell directionality, but it was cultured at a very low flow rate in one channel and did not simulate any diseases.[14] Li et al. observed and measured platelet adhesion for thrombus formation to full occlusion according to shear rates in a multiple channel device.[38] Although a multichannel device was used to achieve a simultaneous comparative and high-throughput analysis of a range of physiological to pathological flow conditions and demonstrated that it can be used to determine patient-specific drug doses; however, there was no cell layer inside the channel and the channel cross-section was rectangular, making it difficult to be considered as an accurate artery model recapitulation.[38,39]

A study of hemodynamics is necessary to understand the mechanisms of arteries and diseases such as atherosclerosis.[36] An alteration in the physical vessel structure through stenosis changes local fluid dynamics such as pressure, velocity, and shear stress, and this also affects platelet adhesion.[34] Therefore, it is essential to understand the relationship between fluid dynamics and arterial disease by creating arterial models of various structures. The effects of various controlled conditions such as geometry and wall shear stress can be analyzed in a parallel and high-throughput manner with a single flow system through the use of a multichannel device.

In this study, human aortic smooth muscle cells (HASMCs) and human umbilical vein endothelial cells (HUVECs) were cocultured in a multichannel device connected with a PDMS fluidic chamber module to fabricate a perfusable 3D in vitro human artery-mimicking multichannel system (Figure 1), particularly mimicking a small muscular artery in which diseases such as thrombosis can occur. To provide directional alignment and contractile morphology to the SMCs, we formed wrinkles on the circular PDMS channel surface as contact guidance, and ECs had directionality through media perfusion. Channels with various geometries and conditions can be easily fabricated by 3D-printed molds to recapitulate various cellular microenvironments and effectively model vessels. Cocultivation models that have tunable and versatile vascular geometries with various diameters, wall shear stress, and types of artery diseases were constructed. Since multiple channels in a device were connected to a PDMS microfluidic chamber module, it was possible to easily control the condition and to fabricate each coculture model in parallel in each channel concurrently. Finally, the effect of the wall shear stress condition depending on the stenotic geometry on cells was compared by a device with four channels with different degrees of stenosis and explored simultaneously. This work highlights the fabrication of an in vivo-like coculture model in a short culture period, the characterization of the coculture model, the identification of protein markers, the multiplexity of models, the microfluidic interfacing, the easy geometrical design, and the relationship between wall shear stress and cells in the in vitro pathologic stenosis model.

2. EXPERIMENTAL SECTION

2.1. Materials. Primary HASMCs and HUVECs were purchased from Lonza (Basel, Switzerland). Red fluorescence protein-expressing human umbilical vein endothelial cells (RFP-HUVECs) were obtained from Angio-Proteomie (Boston, MA, USA). Smooth muscle cell growth medium-2 (SmGM-2) and endothelial cell growth medium-2 (EGM-2) were also supplied from Lonza. Dulbecco's modified Eagle's medium (DMEM) and human plasma fibronectin were obtained from Corning (Corning, NY, USA) and Millipore (Burlington, MA, USA), respectively. Triton X-100 and albumin from bovine serum were bought from Sigma-Aldrich. Normal goat serum was purchase from Vector laboratories (Burlingame, CA, USA). 16% formaldehyde, Hoechst 33342, CellTracker Green CMFDA, and Alexa Fluor 488 Phalloidin were ordered from Thermo Fisher Scientific. Rabbit antialpha smooth muscle actin antibody (ab5694, 1:100), rabbit antismooth muscle myosin heavy chain 11 antibody (ab133567, 1:25), mouse anti-CD31 antibody conjugated with Alexa Fluor 488 (ab215911, 1:100), rabbit anticollagen Type IV antibody (ab6586, 1:100), rabbit antilaminin antibody (ab11575, 1:100), rabbit anti-von Willebrand factor antibody (ab6994, 1:100), goat antirabbit IgG H&L Alexa Fluor 488 (ab150077, 1:200) and goat antirabbit IgG H&L Alexa Fluor 594 (ab150080, 1:200) were obtained from Abcam (Cambridge, UK). A PDMS prepolymer and a curing agent were bought from Dow Corning Corporation (Sylgard 184 elastomer kit; Midland, MI, USA). All stainless steel tubings were obtained from Needle Store (Bucheon, Korea). A white board marker was purchased from Mungyo (Gimhae, Korea). Smooth-Cast 310 liquid plastic was bought from Smooth-On, Inc. (Macungie, PA, USA).

https://dx.doi.org/10.1021/acsbiomaterials.0c00748
ACS Biomater. Sci. Eng. 2020, 6, 5326−5336

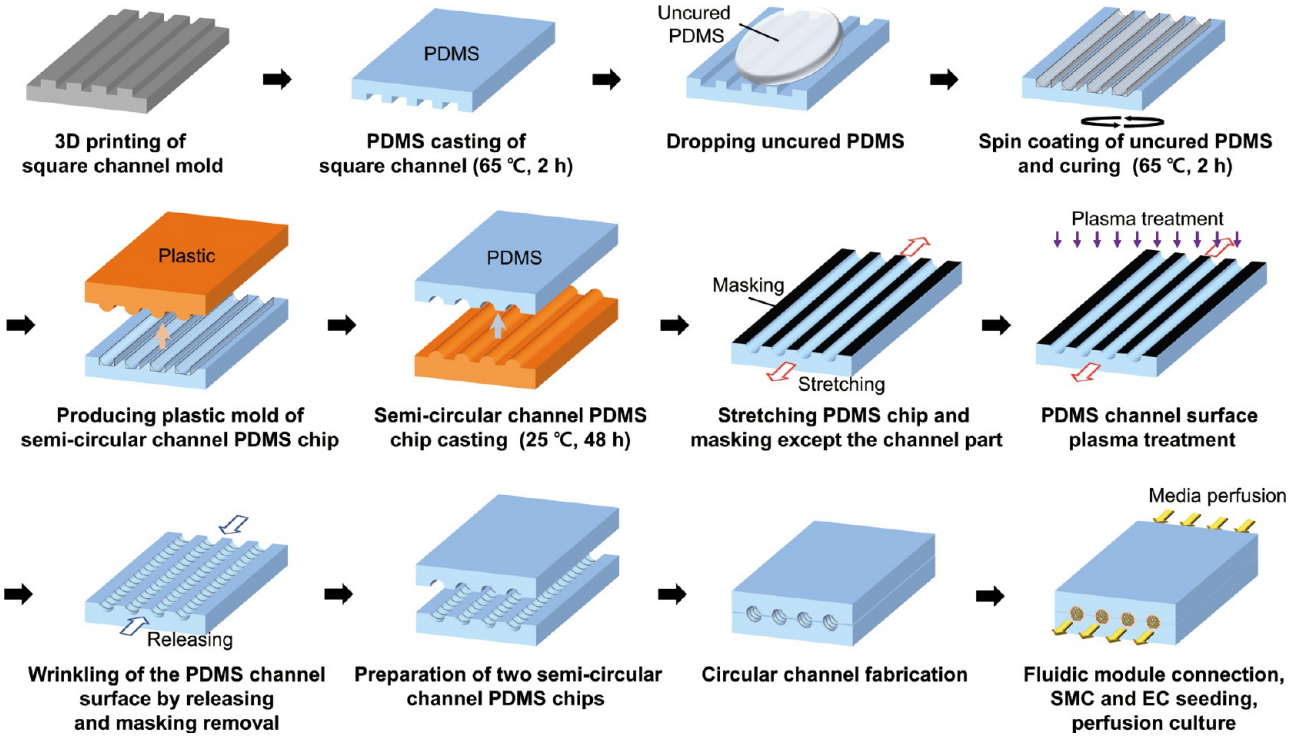

Figure 2. Overall fabrication method of an in vitro artery-mimicking model.

2.2. Fabrication of a 3D In Vitro Artery-Mimicking Circular Multichannel Device. A schematic of a perfusable in vitro artery-mimicking multichannel system is shown in Figure 1 and the overall device fabrication method is described in Figure 2. A device mold with multiple rectangle channels was 3D-printed by PICO2 HD (Asiga, Australia) using PlasCLEAR. After casting PDMS (10:1 = PDMS prepolymer:curing agent) from a 3D-printed mold, 1 mL of uncured PDMS was spin-coated (2000 rpm, 20 s) and cured on the PDMS replica to produce a device with semicircular channels. Smooth-Cast 310 liquid plastic was poured onto the fabricated semicircular channel chip and cured at 25 °C for 24 h then 65 °C for overnight. Produced plastic mold was used semipermanently for casting semicircular channel PDMS chips for further studies. A PDMS device with multiple semicircular channels was casted from the plastic mold and stretched in the axial direction of the channels for 40% using a custom-made clamp, and the surface except the channels was then masked with a marker. Masking was performed to generate wrinkles only in the channel area, otherwise, wrinkles formed in the nonchannel area caused problems in attaching two semicircular channel PDMS chips to fabricate a circular channel chip later. After 30 min of air plasma treatment (2300 cc/min air, 92.5 W, CUTE; Femto Science, Hwaseong, Korea) on the channel surface, the device was released and wrinkles in a circumferential direction of the channels were generated on the channel surface. After removal of masking with Scotch Magic Tape and acetone, two semicircular channel PDMS devices were attached by 1 min plasma treatment. Finally, a device with multiple circular channels was fabricated and fluidic modules were connected through Tygon tubing and stainless steel tubing for perfusion culture of cells. A spin-coating method to fabricate a semicircular channel[40] and a wrinkle generation method in the channel for cellular alignment[41] were referred to previous reports and modified.

2.3. HASMC Culture in Semicircular Channels. To characterize HASMCs by wrinkles on the channel surface, we used semicircular channel devices. The devices were sterilized with 70% ethanol and dried under ultraviolet (UV) exposure. After washing the channels of the devices with phosphate-buffered saline (PBS), the channels were coated with 50 μg/mL human plasma fibronectin in PBS at 37 °C for 1 h. The removal of fibronectin was followed by PBS washing. HASMCs of passage number 5 or 6 in SmGM-2 medium were then seeded at a density of 1×10^5 cells/mL on the device and incubated at 37 °C for 1 h. After 1 h, the channels were washed by SmGM-2 medium and incubated in a humidified incubator at 37 °C. The medium was changed every 24 h, and fluorescence imaging of filamentous actin (F-actin) for the cell orientation angle and cell shape index analysis was performed after 48 h of seeding.

2.4. Coculture of HASMCs and HUVECs in a Multichannel Device. Fluidic modules connected with Tygon and stainless steel tubings and devices with multiple circular channels were sterilized with 70% ethanol and dried under UV exposure. After washing the channels of the devices with PBS, the channels were coated with 50 μg/mL fibronectin in PBS at 37 °C for 1 h. The removal of fibronectin was followed by the connection of devices and fluidic modules. PBS was injected through a fluidic chamber module to wash multiple channels simultaneously. HASMCs of passage number 5 or 6 in SmGM-2 medium were then seeded at a density of 1×10^6 cells/mL into the device and incubated at 37 °C for 30 min. The devices were flipped over and the seeding process was repeated to coat the cells on the entire channel surface. After 30 min, the channels were washed by SmGM-2 medium and incubated in a humidified incubator at 37 °C. The medium was changed every 24 h during 48 h. After 48 h of a static culture of HASMCs, the channels were washed by serum-free DMEM with 1% penicillin−streptomycin. The channels with an HASMC layer were then coated by 50 μg/mL fibronectin in serum-free DMEM at 37 °C for 5 min. The washing of the channels with EGM-2 medium was followed by seeding of HUVECs or RFP-HUVECs of a passage number between 4 and 8 in EGM-2 medium at a density of 4×10^6 cells/mL. After the HUVECs were settled down in a 37 °C incubator for 30 min, the devices were flipped over and the seeding process was repeated. The channels were washed by coculture medium (SmGM-2:EGM-2 = 1:1) and incubated in a humidified incubator at 37 °C. After 24 h of a static coculture, the coculture medium was perfused with 1.8 dyn/cm^2 shear stress per each channel by Minipuls 3 peristaltic pump (Gilson) for 48 h, and immunofluorescence staining of protein markers and extracellular matrices (ECMs) was then performed. For static conditions, the medium was changed every 24 h.

https://dx.doi.org/10.1021/acsbiomaterials.0c00748
ACS Biomater. Sci. Eng. 2020, 6, 5326−5336

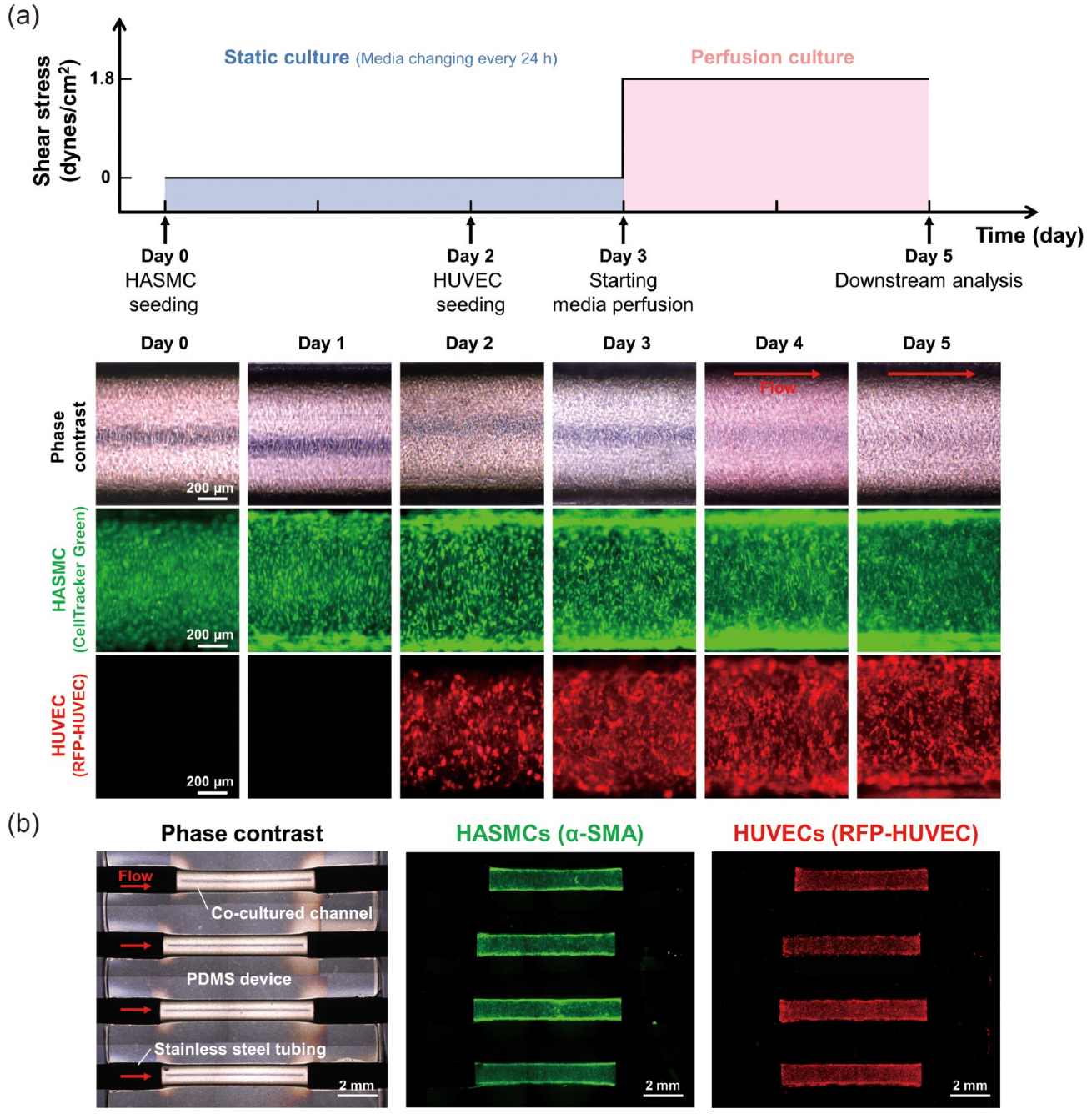

Figure 3. HASMC-HUVEC coculture in a multichannel device. (a) Experimental timeline of producing HASMC-HUVEC coculture model in channels, and corresponding images of cells over time. Over time, cells climbed along the sidewalls and filled the entire channel surface. (b) Phase-contrast, immunofluorescence staining of the HASMC layer, and fluorescence of RFP-HUVEC layer images in a manufactured 3D in vitro artery-mimicking multichannel system after 5 days from the HASMC seeding. Four channels in a device were connected with two PDMS fluidic modules back and forth and controlled together. α-SMA, which is a contractile marker protein of SMC, was stained with immunofluorescence and confirmed the contractility of HASMCs in an in vitro multichannel system.

2.5. Various Designs of Multichannel Artery-Mimicking Model Device. Because of the usage of the 3D-printed mold, the device has versatility on designs and conditions. Numbers, diameters, geometries, and wall shear stress of the channels can be easily controlled by 3D designing of the channel mold. A three-channel device of different diameters, a four-channel device of mimicking different types of artery diseases (healthy, atherosclerosis, aneurysm, and fibromuscular dysplasia), and a four-channel device of different degrees of stenosis each were fabricated and the cells were cocultured in the devices under perfusion flow conditions.

2.6. Von Willebrand Factor Analysis in a Device with Channels of Various Degrees of Stenosis. A device consisting of four channels of 0, 10, 30, and 50% occlusion each was used for simultaneous evaluation of von Willebrand factor (vWF) secretion and accumulation on cells of each model in each channel. A flow rate of 6.35 mL/min was applied to a device and the wall shear stress of each channel was simulated. The vWF fluorescence intensity of the stenosis area in each channel in the static or perfusion environment was compared and analyzed by vWF immunofluorescence staining. By dividing the channel near the stenosis area into five regions (upstream, inlet, apex, outlet, and downstream), we observed the trend of vWF expression for each stenosis channel. Fluorescence images excluding channel edges where the cells were overlapped were used for the analysis.

https://dx.doi.org/10.1021/acsbiomaterials.0c00748
ACS Biomater. Sci. Eng. 2020, 6, 5326−5336

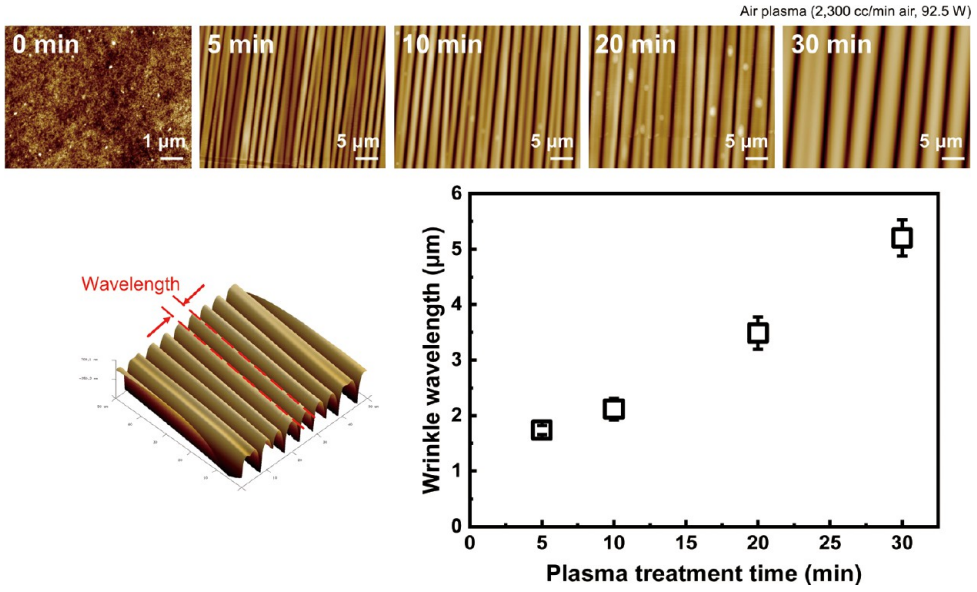

Figure 4. Relationship between wrinkle wavelength and plasma treatment time. AFM images of the PDMS channel surface depend on the plasma treatment time and the graph shows that the longer the plasma treatment time, the longer the wrinkle wavelength. $n = 6$.

2.7. Fluorescence Staining and Imaging. To track and confirm the coculture of HASMCs and HUVECs in an artery-mimicking multichannel system, we stained HASMCs by 2.5 μM CellTracker Green CMFDA in serum-poor DMEM (0.2% fetal bovine serum, 0.1% penicillin−streptomycin) at 37 °C for 15 min, and RFP-HUVECs were used. For the analysis of the HASMCs characteristics, F-actin was stained. HASMCs on semicircular channels were fixed in 4% formaldehyde for 15 min, permeabilized in 0.1% Triton X-100 for 5 min, and stained by 0.165 μM Alexa Fluor 488 Phalloidin for 30 min after 2 days from seeding at room temperature. For the analysis of the HUVEC characteristics and the immunofluorescence staining of protein markers and ECMs, cocultured multichannel models were fixed for 15 min, permeabilized for 10 min, and blocked with 1.5% normal goat serum for 20 min. The cells were immunostained using mouse anti-CD31, rabbit antialpha-smooth muscle actin, rabbit antismooth muscle myosin heavy chain, rabbit anticollagen Type IV, rabbit antilaminin and rabbit anti-vWF monoclonal antibodies, and goat antirabbit IgG. Finally, the nuclei were stained with 5 μg/mL Hoechst 33342 in PBS at room temperature for 10 min. All phase contrast, fluorescence staining, and immunofluorescence staining images were obtained by an inverted microscope (IX51, Olympus), and z-stacked 3D images of HASMCs and HUVECs were visualized by a confocal laser microscope (C2, Nikon) with a z-axis interval of 3 μm. Atomic force microscopic images were obtained by an AFM-Raman spectrometer (INNOVA-LABRAM HR800; Horiba Jobin Yvon, Edison, NJ, USA) in the KAIST Analysis Center for Research Advancement (Daejeon, Korea).

2.8. Computational Simulation of Wall Shear Stress. Finite element analysis (FEA) software, COMSOL Multiphysics (Ver. 5.5, COMSOL Inc.) was used to simulate the wall shear stress of a three-channel device with different diameters and a multichannel stenosis device. The entire device geometries, including the microfluidic chamber modules, were set in full 3D. The medium was assumed to be incompressible water and a fine element mesh was constructed. The laminar flow physics, the inlet boundary condition of the normal inflow velocity, and the outlet boundary condition of the constant atmospheric pressure were applied. The wall shear stress of each channel in a three-channel device with different diameters, and a multichannel stenosis device was calculated and presented as a colored distribution.

3. RESULTS AND DISCUSSION

3.1. Experimental Timeline of HASMC-HUVEC Coculture in a Multichannel Device. The production timeline of an in vitro artery-mimicking multichannel system is shown in Figure 3a. Stretched HASMCs growing in the direction of the circumferential wrinkles on the PDMS channel surface were observed on day 1. HUVECs were seeded in the channels after 48 h of the culture of HASMCs. Seeded HUVECS were stabilized for 1 day and perfusion of media started. Cells that seeded the top and bottom walls of the channel grew up the sidewall and filled the entire channel surface, resulting in the fluorescence intensity of the channel side wall becoming stronger over time. The phase-contrast image of the completed in vitro coculture multichannel system and the fluorescence images of each cell layer are shown in Figure 3b. Alpha-smooth muscle actin (α-SMA) is a major contractile marker indicating that α-SMA expressed HASMCs in this system had a normal contractile phenotype. We produced a perfusable in vitro arterial multichannel system that consisted of a four-channel device in which HASMCs and HUVECs were cocultured and able to test a variety of conditions simultaneously. Since the one device, that is, four channels were connected through one front fluidic chamber module as shown in Figure 1, perfusion culture and parallel assay operation of channels could be easily achieved to create models.

3.2. Characteristics of HASMCs According to the Plasma Treatment Time on the Channel Surface. SMCs are known to grow and orient along the direction of surface micro- and nanostructures of the underneath substrate as contact guidance.[22,42,43] In this study, HASMCs sensed wrinkles on the surface of the PDMS channel as contact guidance, then guided, elongated as a contractile phenotype, and aligned in the wrinkle direction perpendicular to the flow direction as in vivo. The plasma treatment on the stretched PDMS channel creates a hard top oxidized layer on the surface and can cause wrinkles in the perpendicular direction of stretching when released (Figure S1).[44,45] The longer the plasma treatment time, the thicker the oxide layer formed and

https://dx.doi.org/10.1021/acsbiomaterials.0c00748
ACS Biomater. Sci. Eng. 2020, 6, 5326−5336

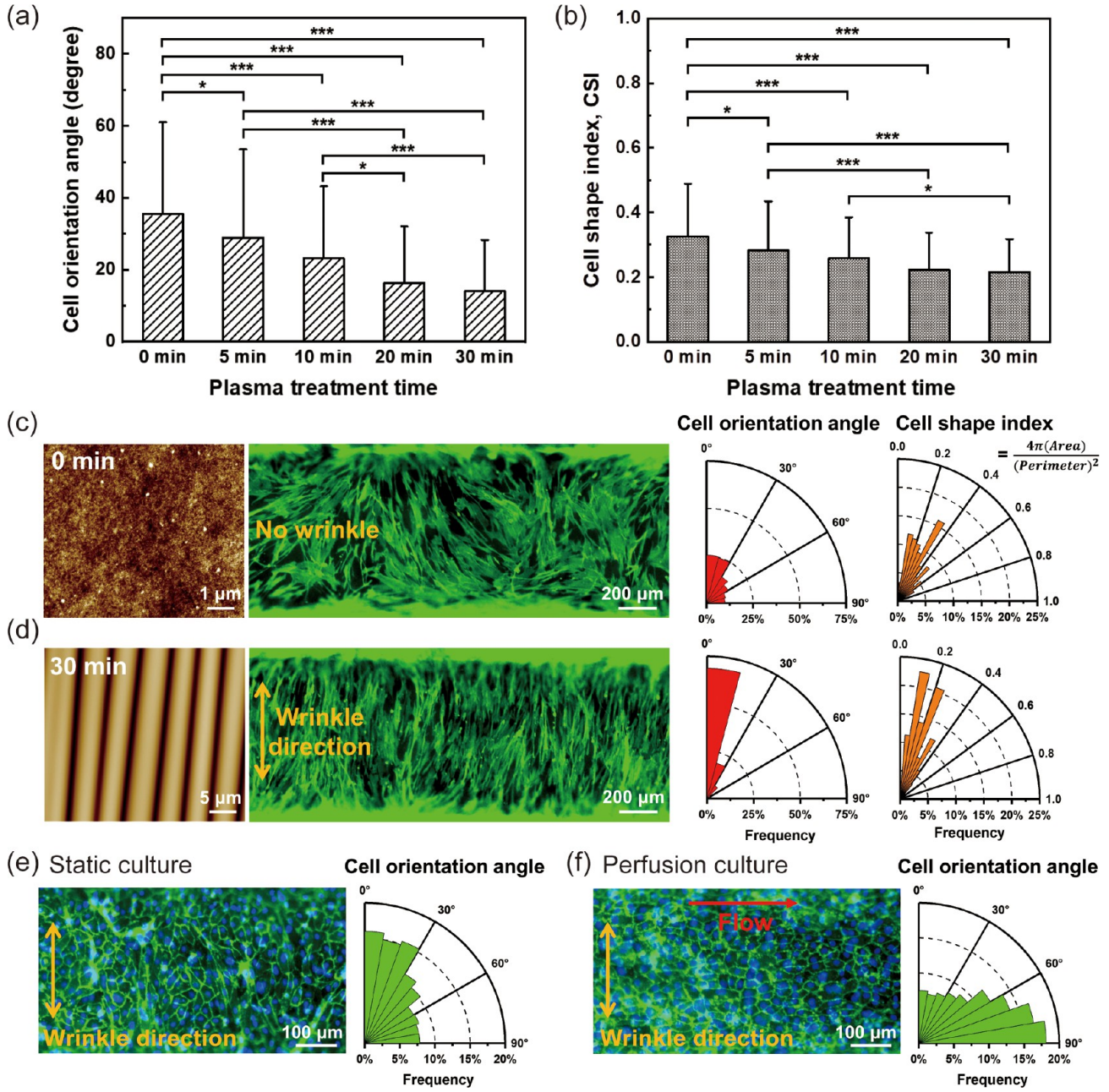

Figure 5. Analysis of circumferentially aligned and stretched HASMCs in a channel and comparison of the morphological characteristics of HUVECs. The effects of plasma treatment time on average (a) OA and (b) CSI of HASMCs. One-way ANOVA with post-hoc Tukey's test (*p < 0.05, ***p < 0.001). Comparison of the morphological characteristics of HASMCs when cells were grown in (c) nonplasma and (d) 30 min plasma-treated channels. AFM images of channel surface, F-actin fluorescence images of HASMCs, OA, and CSI distribution of cells were analyzed. n = 150 cells. Comparison of the morphological characteristics of HUVECs when cells were grown under (e) static and (f) perfusion culture condition. Immunofluorescence staining of CD31 was observed and OA distributions on shear stress were visualized (green, CD31; blue, nuclei). n = 1500 cells.

the larger the wrinkle size according to the image from atomic force microscopy (AFM) (Figure 4).

HASMCs were grown in semicircular PDMS channels with wrinkled surfaces of various sizes. The orientation angle (OA) and the cell shape index (CSI) were evaluated as two indicators to analyze the cell characteristics, directionality and elongation of HASMCs, respectively. The OA is the angle difference between the direction of the cell body and the wrinkle direction. The CSI is an indicator of cell morphology. The closer to 0, the more linear and elongated the cell is, and the closer to 1, the cell is circular. A longer plasma treatment time generated longer wavelength wrinkles, and more HASMCs are aligned in the wrinkle direction (Figure S2), and the mean values of OA and CSI also decrease (Figure 5a, b). The average OA and CSI values of 20 and 30 min treatment showed no significant difference, but when looking at the difference with 10 min, 30 min gave more differences. In this work, to ensure the wrinkle manufacturing process, it was decided to exploit a 30 min plasma treatment in further experiments.

Figure 5c shows that when there was no wrinkle on the surface of the channel, the HASMCs were distributed

https://dx.doi.org/10.1021/acsbiomaterials.0c00748
ACS Biomater. Sci. Eng. 2020, 6, 5326−5336

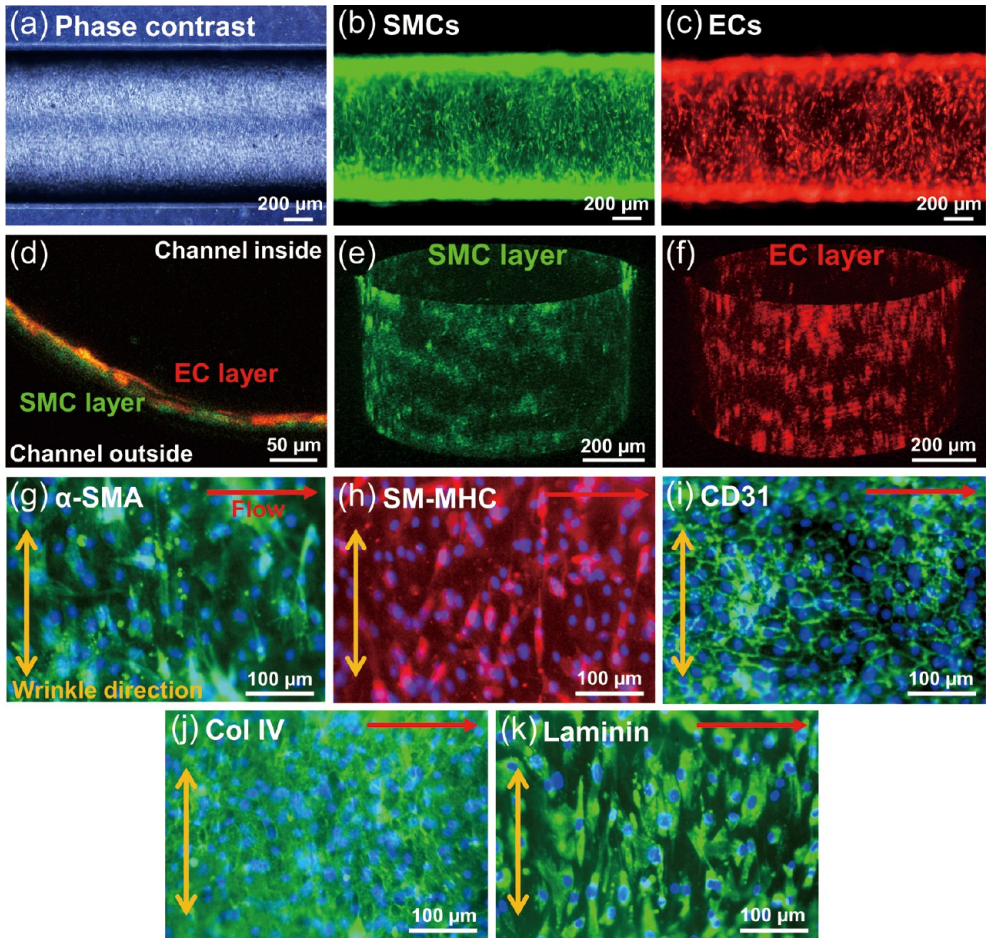

Figure 6. Cocultured SMCs and ECs in an in vitro artery-mimicking model. (a) Phase-contrast image and fluorescent images of (b) SMC layer (CellTracker Green) and (c) EC layer (RFP-HUVEC) of the model. (d) Stacked cell layers were confirmed in the cross-section image of the coculture model. 3D *z*-stacked images of (e) SMC and (f) EC layer (green, CellTracker Green; red, RFP-HUVEC). Immunofluorescence staining images of protein markers of (g, h) SMC (*α*-SMA, SM-MHC), (i) EC (CD31), and synthesized ECMs (j) Col IV, (k) laminin in the model (green and red, each marker; blue, nuclei).

somewhat evenly, and only 25.3% of the cells had an OA of 0−15°. However, most of the HASMCs (68.7%) represented an OA of 0−15° and were aligned along with the wrinkles, when cultured in channels with 30 min plasma treatment, resulting in wrinkles with an average wavelength of 5.20 μm (Figure 5d). Aligned cells were 2.71-fold higher population compared to the culture in the channel with 0 min treatment. Even 88.0% of the HASMCs existed within an OA range of 0−30°. We also see that SMCs had a lower CSI value of 0.215 on average, which means they are more elongated and had contractile spindle shapes in the wrinkled channel. We confirmed that the HASMC layer was aligned in the circumferential orientation and elongated as a contractile phenotype as an in vivo state in the wrinkled-surface channel.

3.3. Characteristics of HUVECs Depending on the Shear Stress. We compared the HUVEC morphology change in the coculture model for the condition with shear stress to the static state (Figure 5e, f). ECs of a native artery are exposed to shear stress, the physical force due to blood flow. ECs sense the shear stress and are aligned in the direction of flow.[20,23] CD31, an endothelial cell intercellular junction protein, was stained and analyzed with immunofluorescence. The CD31 staining showed good cell junctions and a confluent HUVEC monolayer under both static and perfusion culture conditions. HUVECs were also affected by the topography underneath.[46] Therefore, most HUVECs were generally circumferentially aligned in the absence of flow because the lower HASMC layer was stretched and aligned along with the wrinkles (Figure 5e). When the 1.8 dyn/cm^2 of shear stress was applied by the media flow, the HUVECs were rearranged and showed elongated morphology parallel to the fluid direction as in vivo (Figure 5f). The cell body angle difference with the wrinkle direction was also defined as the orientation angle for the HUVECs, which means that 90° is cells aligned in the flow direction. In perfusion compared to the static condition, the frequency of cells aligned in the flow direction with an angle of 80−90° increased from 7.87 to 18.1% or 2.31 times. The frequency of cells aligned in the wrinkle direction with an angle of 0−10° decreased 2.12 times from 15.9 to 7.53%. Another junction protein, vascular endothelial cadherin (VE-Cad), was also stained and observed (data not shown). As a result, endothelial cell intercellular junction marker CD31 staining confirmed that the ECs were aligned in the flow direction and formed a confluent monolayer on the SMC layer in the perfused coculture model as in vivo.

3.4. Coculture of HASMCs and HUVECs in a Perfusable In Vitro Artery-Mimicking Multichannel Device. An in vitro arterial multichannel model was developed to test various conditions simultaneously. The HASMC−HUVEC coculture model in a perfusable in vitro artery-

https://dx.doi.org/10.1021/acsbiomaterials.0c00748
ACS Biomater. Sci. Eng. 2020, 6, 5326−5336

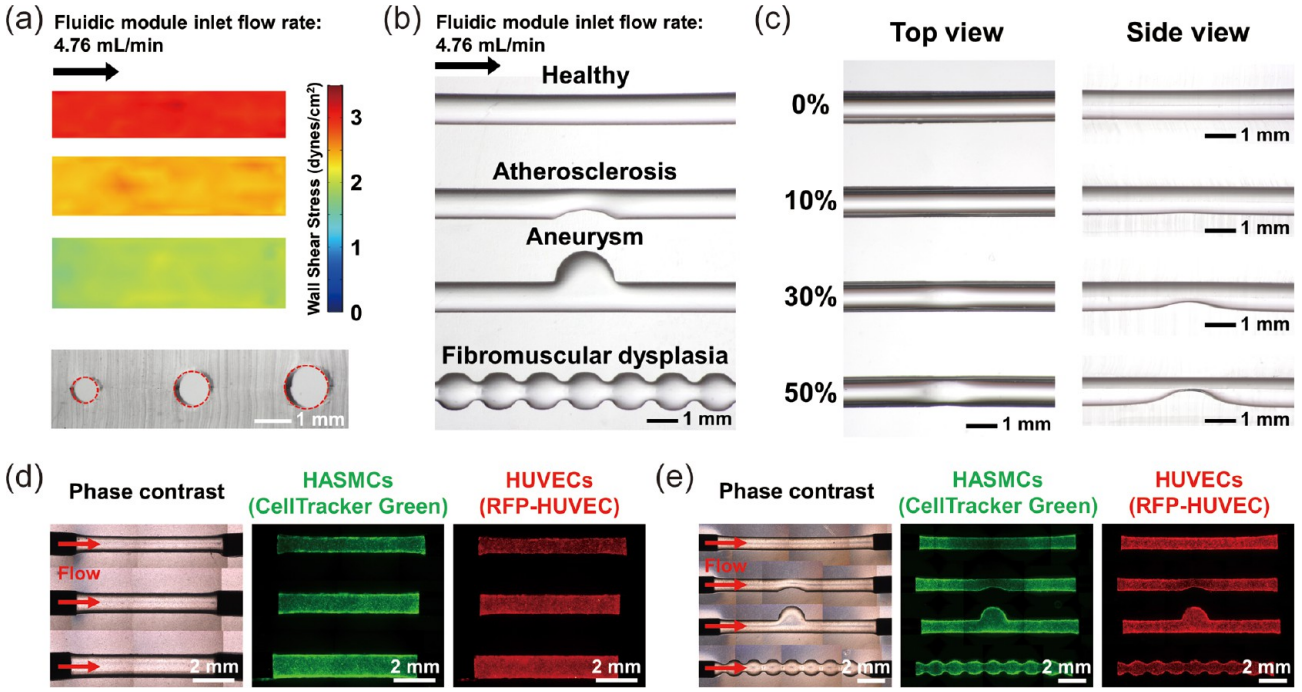

Figure 7. Versatility in a developed perfusable in vitro artery-mimicking multichannel device. Diverse channel numbers, channel diameters, channel geometries, and wall shear stress were realized, and the cells were perfusion cocultured in the device. (a) Three-channel device with different diameters for each channel. Top: the wall shear stress of each channel with 800, 1000, and 1200 μm diameter in a device was simulated. Bottom: the cross-section of the fabricated PDMS channel device was shown. (b) In vivo geometries of diseased arteries were recapitulated in vitro by 3D designing and printing of the channel mold. Each channel of a four-channel device mimicked different types of artery diseases (healthy, atherosclerosis, aneurysm, and fibromuscular dysplasia). (c) Device of four channels with different degrees of stenosis. Phase-contrast image and fluorescence images of HASMC and HUVEC layers of the cocultured model in (d) a three-channel device with different diameters and (e) a diseased artery recapitulating device. Each cell layer in the cocultured model was well identified.

mimicking multichannel device was formed by seeding first SMCs and then ECs on the top in four multichannels. Four channels were connected through the fluidic chamber as shown in Figure 1, allowing four coculture channels to grow in parallel. As a result, cells were cocultured in a wrinkled-surface PDMS multichannel device to fabricate models in parallel that were composed of circumferentially aligned SMCs with elongated contractile phenotypes and confluent and axially aligned ECs as in vivo. Each cell layer was identified by fluorescence staining (Figure 6a–c), and the cross-section (Figure 6d) and the 3D z-stacked image (Figure 6e and f) confirmed well-stacked layers of the model. The cocultured cells in the multichannel device were examined by immunofluorescence staining to determine whether each cell secreted characteristic markers and whether basal lamina ECM proteins were well synthesized. The α-SMA and smooth muscle myosin heavy chain (SM-MHC) produced by SMCs contributes to the vessel's function as a contractile marker. The staining of α-SMA (Figure 6g), SM-MHC (Figure 6h), and CD31 (Figure 6i) revealed that HASMCs had contractility, and HUVECs formed a good junction and a confluent layer in a cocultured multichannel system, respectively. HASMCs cocultured with HUVECs express more α-SMA than HASMCs monocultured in a device, and it was confirmed that HASMCs were more contractile when cocultured with HUVECs (Figure S3). We could also obtain orientation information on cells in which the HASMCs were perpendicular to the channel axis and the HUVECs were in the axial direction. The synthesis of ECM proteins by cells is an essential component of cellular functionality in building in vitro models. Immunofluorescence staining identified the production and secretion of major components of basal lamina ECM proteins of native vessels, collagen Type IV (Col IV), which spread like a net with a fibrous structure (Figure 6j), and laminin (Figure 6k).

3.5. Design and Condition Versatility of the Multichannel Device. A 3D-printed mold reduced limits with model design and condition in the manufacture of a versatile 3D in vitro artery-mimicking multichannel device. Effectively recapitulated complex 3D microenvironments and physiological conditions by the production of a well-ordered model show the potential for further cell-based assays. Three types of multichannel devices were produced: (1) devices with various diameters and shears (Figure 7a), (2) devices mimicking various artery diseases (Figure 7b), (3) stenosis devices with geometrical differences (Figure 7c). The device with various diameters and shears consists of three channels in one device, and each channel has a different diameter. The wall shear stress applied to each channel was observed through the simulation, and it was confirmed by fluorescence photography that HASMCs and HUVECs were well cocultured under different shear stresses to form a model (Figure 7d). Next, the four-channel device mimicking geometries of various artery diseases were constructed. Each channel in a device has the shape of a healthy, atherosclerosis, aneurysm, and fibromuscular dysplasia artery, and each cell layer was well presented inside the channel (Figure 7e). A stenosis device with geometrical differences was also fabricated to analyze vWF expression aspects. Wrinkles were well generated (Figure S4a) and HASMCs and HUVECs were circumferentially and axially aligned, respectively, in the stenosis region (Figure S4b, c) under perfusion culture

https://dx.doi.org/10.1021/acsbiomaterials.0c00748
ACS Biomater. Sci. Eng. 2020, 6, 5326–5336

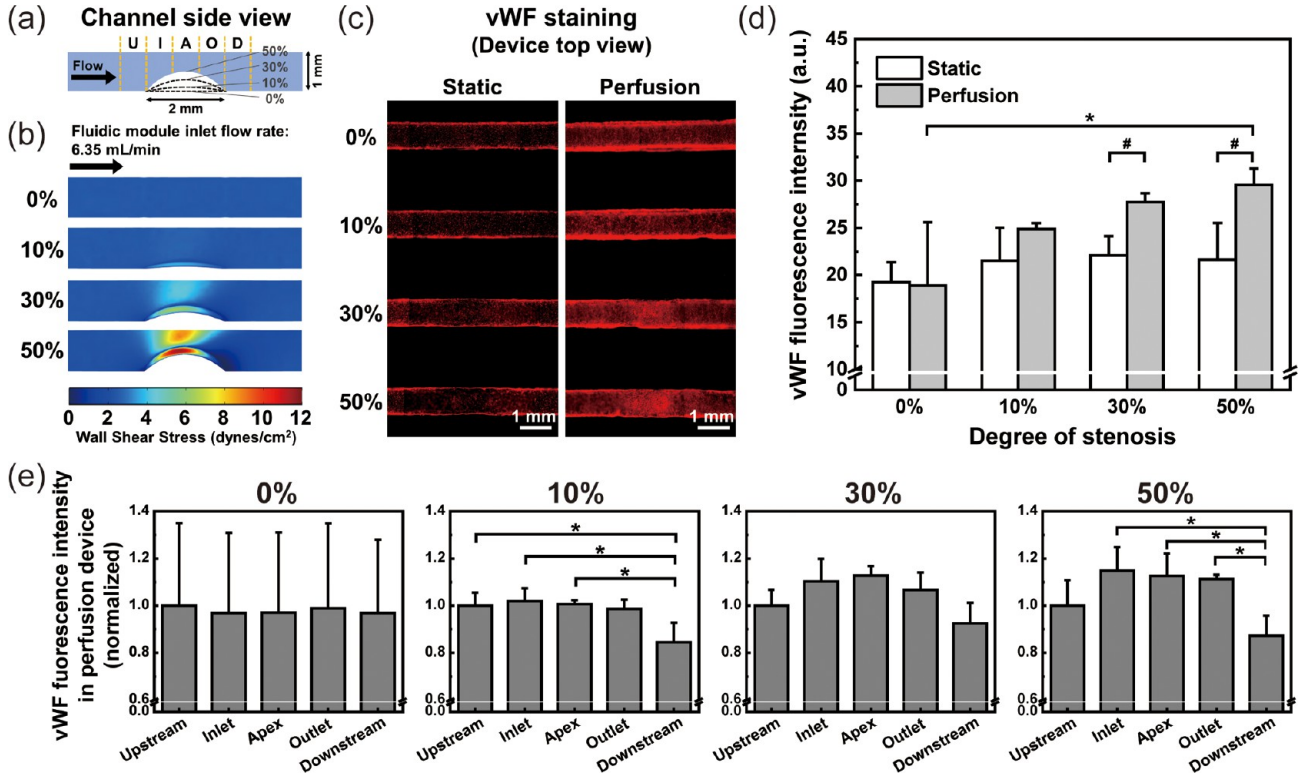

Figure 8. vWF expression in the multichannel stenosis device. (a) Channel area near the stenosis was divided into five regions (U, upstream; I, inlet; A, apex; O, outlet; D, downstream) for analysis. The channel side view scheme shows the design and dimension of the stenosis channels. (b) Wall shear stress of each channel with 0, 10, 30, and 50% occlusion in a device was simulated and a perspective view was shown. (c) vWF immunofluorescence staining micrographs of a multichannel device with four different degrees of stenosis channels in the static or perfusion environment. (d) vWF expression in the stenosis area of each channel in the static or perfusion environment was compared by staining. One-way ANOVA with post-hoc Tukey's test (*$p < 0.05$) in vWF fluorescence intensities among degrees of stenosis. Student's t-test (#$p < 0.05$) at the same degree of stenosis whether it was in a static or a perfusion state. $n = 3$. (e) Trend of vWF expression for each stenosis channel in a device by dividing the stenosis area into five different regions was valued. The intensity values were normalized to the values of the channel upstream in each degree of stenosis. One-way ANOVA with post-hoc Tukey's test (*$p < 0.05$). $n = 3$.

condition, making this stenosis device a suitable model for analysis. As such, a multichannel device with tunable vascular geometries and on-demand multiplexing could be easily fabricated, and coculture models in multiple channels existed in parallel in the device. Because the alteration of geometry leads to changes in local hemodynamics such as velocity, stress, and pressure, it can be used as a model that recapitulates the pathophysiology of in vivo disease and has the potential to be used as a platform for comparison and experiment with multiple conditions simultaneously.

3.6. vWF Expression in a Stenosis Device. vWF is an adhesive glycoprotein that is involved in platelet adhesion, hemostasis, and thrombus formation in blood vessels.[35,47] Shear stress can induce the secretion of vWF from ECs, thereby promoting platelet adhesion and aggregation.[48,49] Through the stenosis structure of the multichannel device, the local hemodynamic conditions in the channel were changed, and the effect of the wall shear stress on the vWF secretion of the ECs was examined (Figure 8). Four channels with 0, 10, 30, and 50% occlusion coexisted in one device and each stenotic geometry was located at the bottom of the channel (Figure 8a). We simultaneously applied four stenotic wall shear stress conditions within each of the four stenotic channels with different degrees of stenosis in a device. A single flow system with multiple conditions such as stenotic geometries and wall shear stress was able to perform a controlled, comparative, parallel, and high-throughput simultaneous analysis. The wall shear stress applied to each stenotic channel in a device was calculated by COMSOL simulation (Figure 8b). HASMCs and HUVECs were cocultured in a stenotic multichannel model. According to the vWF staining, there was no statistically significant difference in the vWF expression level with respect to the degree of stenosis under static culture conditions (Figure 8c, d). Under perfusion culture conditions, the applied local shear stress increased with increasing degree of stenosis, and thus the vWF secretion level of the stenotic region was stimulated and increased (Figure 8c, d). As the degree of stenosis increased, the signal difference between static and perfusion conditions with the same degree of stenosis significantly increased, and the signal difference from nonstenotic channels also significantly increased within the perfusion model. This result was consistent with previous research that vWF synthesis was modulated when HUVEC was exposed to physical stimulation, shear stress.[35,48,49]

In the case of perfusion conditions, the tendency of vWF expression was observed by dividing the area near the stenosis into five regions (Figure 8a, e). The normalized fluorescence intensity of each region to the intensity of the upstream region in each stenosis channel showed that there was no significant difference in the signal of all regions in the nonstenotic channel, but the signal of the stenosis region (inlet, apex, and outlet) increased as the degree of stenosis increased. In the 50% stenotic channel, the vWF intensity of the inlet and apex regions was elevated with high wall shear stress as in a

https://dx.doi.org/10.1021/acsbiomaterials.0c00748
ACS Biomater. Sci. Eng. 2020, 6, 5326−5336

simulation result. Through the four-channel stenosis model, only the effect of shear stress, which was independent of various external environmental factors, on coculture models could be directly controlled and compared simultaneously in parallel from the normal to the pathological channel. Although the wall shear stress range of this system was slightly lower than the physiological and pathological range of the actual artery, changes in vWF expression of cells due to stenosis were demonstrated. Further studies adapting the system to a more physiological environment with the use of appropriate equipment and improving the front-mounted microfluidic module will improve this system to be used as a platform for the screening of antiplatelet drugs of an atherosclerosis model.

4. CONCLUSIONS

This paper presents the fabrication of a perfusable 3D in vitro artery-mimicking multichannel system by coculture of HASMCs and HUVECs in a multichannel device connected with PDMS fluidic chamber modules. The circumferential alignment and spindle-shaped contractile morphology of HASMCs were satisfied by the wrinkle structure on the circular PDMS channel surface as contact guidance, and a confluent HUVEC layer has directionality through media perfusion in the coculture model. The versatility in geometries and conditions and on-demand multiplexing of the channel was obtained by 3D printing of the channel mold to recapitulate various cellular microenvironments and effectively model vessels. Finally, to study the effect of wall shear stress on models, we developed a multichannel device consisting of four channels with different degrees of stenosis to characterize the mechano-regulation of vWF of models across various shear ranges. Because multiple channels in a device were connected to one front PDMS microfluidic chamber module, it was easy to control the conditions, fabricate each coculture model in each channel parallelly, and examine the results simultaneously. Owing to the device interfacing with a microfluidic module, this artery-on-a-chip model has the potential to comprehensively investigate various conditions of vascular diseases simultaneously along with the microfluidics improvement in the context of vascular geometries.

■ ASSOCIATED CONTENT

Supporting Information

The Supporting Information is available free of charge at https://pubs.acs.org/doi/10.1021/acsbiomaterials.0c00748.

Wrinkle structure generation procedure on the PDMS channel surface (Figure S1); cell orientation angle distribution graphs of HASMCs cultured in a semicircular channel device (Figure S2); α-SMA expression of HASMCs cocultured with HUVECs and HASMCs monocultured in a device (Figure S3); images of wrinkles and cells in the stenosis channel (Figure S4) (PDF)

■ AUTHOR INFORMATION

Corresponding Author

Je-Kyun Park − *Department of Bio and Brain Engineering, Korea Advanced Institute of Science and Technology (KAIST), Daejeon 34141, Republic of Korea; KAIST Institute for Health Science and Technology, Daejeon 34141, Republic of Korea;* orcid.org/0000-0003-4522-2574; Phone: +82-42-350-4315; Email: jekyun@kaist.ac.kr; Fax: +82-42-350-4310

Author

Minkyung Cho − *Department of Bio and Brain Engineering, Korea Advanced Institute of Science and Technology (KAIST), Daejeon 34141, Republic of Korea*

Complete contact information is available at: https://pubs.acs.org/10.1021/acsbiomaterials.0c00748

Notes

The authors declare no competing financial interest.

■ ACKNOWLEDGMENTS

This work was supported by the National Research Foundation of Korea (NRF) funded by the Korean government (MSIT) (NRF-2019R1A2B5B03070494 and NRF-2015M3A9B3028685).

■ REFERENCES

(1) Swirski, F. K.; Nahrendorf, M. Leukocyte Behavior in Atherosclerosis, Myocardial Infarction, and Heart Failure. *Science* **2013**, *339*, 161−166.

(2) Lee, R. T.; Libby, P. The Unstable Atheroma. *Arterioscler., Thromb., Vasc. Biol.* **1997**, *17*, 1859−1867.

(3) Ross, R. The Pathogenesis of Atherosclerosis: A Perspective for the 1990s. *Nature* **1993**, *362*, 801−809.

(4) Libby, P. Mechanisms of Acute Coronary Syndromes and Their Implications for Therapy. *N. Engl. J. Med.* **2013**, *368*, 2004−2013.

(5) Fuster, V.; Lewis, A. Conner Memorial Lecture. Mechanisms Leading to Myocardial Infarction: Insights from Studies of Vascular Biology. *Circulation* **1994**, *90*, 2126−2146.

(6) Dunphy, M. P.; Strauss, H. W. The Pathology of Atherosclerosis. In *Imaging of Carotid Artery Stenosis*; Schaller, B. J., Ed.; Springer Vienna: Vienna, Austria, 2007; pp 7−18.

(7) Janke, D.; Jankowski, J.; Rüth, M.; Buschmann, I.; Lemke, H.-D.; Jacobi, D.; Knaus, P.; Spindler, E.; Zidek, W.; Lehmann, K.; Jankowski, V. The "Artificial Artery" as In Vitro Perfusion Model. *PLoS One* **2013**, *8*, No. e57227.

(8) Shinohara, S.; Kihara, T.; Sakai, S.; Matsusaki, M.; Akashi, M.; Taya, M.; Miyake, J. Fabrication of In Vitro Three-Dimensional Multilayered Blood Vessel Model Using Human Endothelial and Smooth Muscle Cells and High-Strength PEG Hydrogel. *J. Biosci. Bioeng.* **2013**, *116*, 231−234.

(9) Mannino, R. G.; Myers, D. R.; Ahn, B.; Wang, Y.; Rollins, M.; Gole, H.; Lin, A. S.; Guldberg, R. E.; Giddens, D. P.; Timmins, L. H.; Lam, W. A. Do-It-Yourself In Vitro Vasculature that Recapitulates In Vivo Geometries for Investigating Endothelial-Blood Cell Interactions. *Sci. Rep.* **2015**, *5*, 12401.

(10) Sebastian, B.; Dittrich, P. S. Microfluidics to Mimic Blood Flow in Health and Disease. *Annu. Rev. Fluid Mech.* **2018**, *50*, 483−504.

(11) Costa, P. F.; Albers, H. J.; Linssen, J. E. A.; Middelkamp, H. H. T.; van der Hout, L.; Passier, R.; van den Berg, A.; Malda, J.; van der Meer, A. D. Mimicking Arterial Thrombosis in a 3D-Printed Microfluidic In Vitro Vascular Model based on Computed Tomography Angiography Data. *Lab Chip* **2017**, *17*, 2785−2792.

(12) Hachey, S. J.; Hughes, C. C. W. Applications of Tumor Chip Technology. *Lab Chip* **2018**, *18*, 2893−2912.

(13) Fiddes, L. K.; Raz, N.; Srigunapalan, S.; Tumarkan, E.; Simmons, C. A.; Wheeler, A. R.; Kumacheva, E. A Circular Cross-Section PDMS Microfluidics System for Replication of Cardiovascular Flow Conditions. *Biomaterials* **2010**, *31*, 3459−3464.

(14) Choi, J. S.; Seo, T. S. Orthogonal Co-Cultivation of Smooth Muscle Cell and Endothelial Cell Layers to Construct In Vivo-like Vasculature. *Biomicrofluidics* **2019**, *13*, 014115.

(15) Sfriso, R.; Zhang, S.; Bichsel, C. A.; Steck, O.; Despont, A.; Guenat, O. T.; Rieben, R. 3D Artificial Round Section Micro-Vessels to Investigate Endothelial Cells Under Physiological Flow Conditions. *Sci. Rep.* **2018**, *8*, 1−13.

(16) Tan, A.; Fujisawa, K.; Yukawa, Y.; Matsunaga, Y. T. Bottom-Up Fabrication of Artery-Mimicking Tubular Co-Cultures in Collagen-based Microchannel Scaffolds. *Biomater. Sci.* **2016**, *4*, 1503−1514.
(17) Pitingolo, G.; Vecchione, R.; Falanga, A. P.; Guarnieri, D.; Netti, P. A. Fabrication of a Modular Hybrid Chip to Mimic Endothelial-lined Microvessels in Flow Conditions. *J. Micromech. Microeng.* **2017**, *27*, 035014.
(18) Ye, G. J. C.; Aratyn-Schaus, Y.; Nesmith, A. P.; Pasqualini, F. S.; Alford, P. W.; Parker, K. K. The Contractile Strength of Vascular Smooth Muscle Myocytes is Shape Dependent. *Integr. Biol.* **2014**, *6*, 152−163.
(19) Chang, S.; Song, S.; Lee, J.; Yoon, J.; Park, J.; Choi, S.; Park, J.-K.; Choi, K.; Choi, C. Phenotypic Modulation of Primary Vascular Smooth Muscle Cells by Short-term Culture on Micropatterned Substrate. *PLoS One* **2014**, *9*, No. e88089.
(20) Li, Y.; Huang, G.; Zhang, X.; Wang, L.; Du, Y.; Lu, T. J.; Xu, F. Engineering Cell Alignment In Vitro. *Biotechnol. Adv.* **2014**, *32*, 347−365.
(21) Rhodin, J. A. G. Architecture of the Vessel Wall. In *Handbook of Physiology: The Cardiovascular System II*; American Physiological Society: Rockville, MD, 1977; Vol. *2*, pp 1−31.
(22) Xu, C. Y.; Inai, R.; Kotaki, M.; Ramakrishna, S. Aligned Biodegradable Nanofibrous Structure: A Potential Scaffold for Blood Vessel Engineering. *Biomaterials* **2004**, *25*, 877−886.
(23) Paszkowiak, J. J.; Dardik, A. Arterial Wall Shear Stress: Observations from the Bench to the Bedside. *Vasc. Endovascular Surg.* **2003**, *37*, 47−57.
(24) L'Heureux, N.; Germain, L.; Labbé, R.; Auger, F. A. In Vitro Construction of a Human Blood Vessel from Cultured Vascular Cells: A Morphologic Study. *J. Vasc. Surg.* **1993**, *17*, 499−509.
(25) Syedain, Z. H.; Meier, L. A.; Bjork, J. W.; Lee, A.; Tranquillo, R. T. Implantable Arterial Grafts from Human Fibroblasts and Fibrin using a Multi-Graft Pulsed Flow-Stretch Bioreactor with Noninvasive Strength Monitoring. *Biomaterials* **2011**, *32*, 714−722.
(26) Aper, T.; Wilhelmi, M.; Gebhardt, C.; Hoeffler, K.; Benecke, N.; Hilfiker, A.; Haverich, A. Novel Method for the Generation of Tissue-Engineered Vascular Grafts based on a Highly Compacted Fibrin Matrix. *Acta Biomater.* **2016**, *29*, 21−32.
(27) Ju, Y. M.; Choi, J. S.; Atala, A.; Yoo, J. J.; Lee, S. J. Bilayered Scaffold for Engineering Cellularized Blood Vessels. *Biomaterials* **2010**, *31*, 4313−4321.
(28) Cheng, S.; Jin, Y.; Wang, N.; Cao, F.; Zhang, W.; Bai, W.; Zheng, W.; Jiang, X. Self-Adjusting, Polymeric Multilayered Roll that can Keep the Shapes of the Blood Vessel Scaffolds during Biodegradation. *Adv. Mater.* **2017**, *29*, 1700171.
(29) Liu, Y.; Lu, J.; Li, H.; Wei, J.; Li, X. Engineering Blood Vessels through Micropatterned Co-Culture of Vascular Endothelial and Smooth Muscle Cells on Bilayered Electrospun Fibrous Mats with pDNA Inoculation. *Acta Biomater.* **2015**, *11*, 114−125.
(30) Yuan, B.; Jin, Y.; Sun, Y.; Wang, D.; Sun, J.; Wang, Z.; Zhang, W.; Jiang, X. A Strategy for Depositing Different Types of Cells in Three Dimensions to Mimic Tubular Structures in Tissues. *Adv. Mater.* **2012**, *24*, 890−896.
(31) Weinberg, C. B.; Bell, E. A Blood Vessel Model Constructed from Collagen and Cultured Vascular Cells. *Science* **1986**, *231*, 397−400.
(32) Liu, D.; Xiang, T.; Gong, T.; Tian, T.; Liu, X.; Zhou, S. Bioinspired 3D Multilayered Shape Memory Scaffold with a Hierarchically Changeable Micropatterned Surface for Efficient Vascularization. *ACS Appl. Mater. Interfaces* **2017**, *9*, 19725−19735.
(33) Jung, Y.; Ji, H.; Chen, Z.; Fai Chan, H.; Atchison, L.; Klitzman, B.; Truskey, G.; Leong, K. W. Scaffold-Free, Human Mesenchymal Stem Cell-based Tissue Engineered Blood Vessels. *Sci. Rep.* **2015**, *5*, 15116.
(34) Yamagishi, Y.; Masuda, T.; Matsusaki, M.; Akashi, M.; Yokoyama, U.; Arai, F. Microfluidic Perfusion Culture System for Multilayer Artery Tissue Models. *Biomicrofluidics* **2014**, *8*, 064113.
(35) Westein, E.; van der Meer, A. D.; Kuijpers, M. J. E.; Frimat, J.-P.; van den Berg, A.; Heemskerk, J. W. M. Atherosclerotic Geometries Exacerbate Pathological Thrombus Formation Poststenosis in a von Willebrand Factor-dependent Manner. *Proc. Natl. Acad. Sci. U. S. A.* **2013**, *110*, 1357−1362.
(36) Korin, N.; Kanapathipillai, M.; Matthews, B. D.; Crescente, M.; Brill, A.; Mammoto, T.; Ghosh, K.; Jurek, S.; Bencherif, S. A.; Bhatta, D.; Coskun, A. U.; Feldman, C. L.; Wagner, D. D.; Ingber, D. E. Shear-Activated Nanotherapeutics for Drug Targeting to Obstructed Blood Vessels. *Science* **2012**, *337*, 738−742.
(37) Venugopal Menon, N.; Tay, H. M.; Pang, K. T.; Dalan, R.; Wong, S. C.; Wang, X.; Li, K. H. H.; Hou, H. W. A Tunable Microfluidic 3D Stenosis Model to Study Leukocyte-Endothelial Interactions in Atherosclerosis. *APL Bioeng.* **2018**, *2*, 016103.
(38) Li, M.; Ku, D. N.; Forest, C. R. Microfluidic System for Simultaneous Optical Measurement of Platelet Aggregation at Multiple Shear Rates in Whole Blood. *Lab Chip* **2012**, *12*, 1355−1362.
(39) Li, M.; Hotaling, N. A.; Ku, D. N.; Forest, C. R. Microfluidic Thrombosis Under Multiple Shear Rates and Antiplatelet Therapy Doses. *PLoS One* **2014**, *9*, No. e82493.
(40) Vecchione, R.; Pitingolo, G.; Guarnieri, D.; Falanga, A. P.; Netti, P. A. From Square to Circular Polymeric Microchannels by Spin Coating Technology: A Low Cost Platform for Endothelial Cell Culture. *Biofabrication* **2016**, *8*, 025005.
(41) Choi, J. S.; Piao, Y.; Seo, T. S. Circumferential Alignment of Vascular Smooth Muscle Cells in a Circular Microfluidic Channel. *Biomaterials* **2014**, *35*, 63−70.
(42) Shen, J. Y.; Chan-Park, M. B.; He, B.; Zhu, A. P.; Zhu, X.; Beuerman, R. W.; Yang, E. B.; Chen, W.; Chan, V. Three-dimensional Microchannels in Biodegradable Polymeric Films for Control Orientation and Phenotype of Vascular Smooth Muscle Cells. *Tissue Eng.* **2006**, *12*, 2229−2240.
(43) Cao, Y.; Poon, Y. F.; Feng, J.; Rayatpisheh, S.; Chan, V.; Chan-Park, M. B. Regulating Orientation and Phenotype of Primary Vascular Smooth Muscle Cells by Biodegradable Films Patterned with Arrays of Microchannels and Discontinuous Microwalls. *Biomaterials* **2010**, *31*, 6228−6238.
(44) Yang, S.; Khare, K.; Lin, P. C. Harnessing Surface Wrinkle Patterns in Soft Matter. *Adv. Funct. Mater.* **2010**, *20*, 2550−2564.
(45) Nania, M.; Foglia, F.; Matar, O. K.; Cabral, J. T. Sub-100 nm Wrinkling of Polydimethylsiloxane by Double Frontal Oxidation. *Nanoscale* **2017**, *9*, 2030−2037.
(46) Liliensiek, S. J.; Wood, J. A.; Yong, J.; Auerbach, R.; Nealey, P. F.; Murphy, C. J. Modulation of Human Vascular Endothelial Cell Behaviors by Nanotopographic Cues. *Biomaterials* **2010**, *31*, 5418−5426.
(47) Qiu, Y.; Ciciliano, J.; Myers, D. R.; Tran, R.; Lam, W. A. Platelets and Physics: How Platelets "Feel" and Respond to their Mechanical Microenvironment. *Blood Rev.* **2015**, *29*, 377−386.
(48) Galbusera, M.; Zoja, C.; Donadelli, R.; Paris, S.; Morigi, M.; Benigni, A.; Figliuzzi, M.; Remuzzi, G.; Remuzzi, A. Fluid Shear Stress Modulates von Willebrand Factor Release from Human Vascular Endothelium. *Blood* **1997**, *90*, 1558−1564.
(49) Sun, R. J.; Muller, S.; Wang, X.; Zhuang, F. Y.; Stoltz, J. F. Regulation of von Willebrand Factor of Human Endothelial Cells Exposed to Laminar Flows: An In Vitro Study. *Clin. Hemorheol. Microcirc.* **2000**, *23*, 1−11.

https://dx.doi.org/10.1021/acsbiomaterials.0c00748
ACS Biomater. Sci. Eng. 2020, 6, 5326−5336